STRUCTURAL EVOLUTION OF SUPER ALPHA-TWO Ti₃Al POWDER BALL MILLED IN AIR

Th. Kehagias, Ph. Komninou, P. Kavouras, E. Sarigiannidou, S. Kokkou, J.G. Antonopoulos and Th. Karakostas

Aristotle University, Department of Physics, 540 06 Thessaloniki, Greece

G. Nouet

LERMAT, UPRESA CNRS 6004, ISMRA, 6 Bd. du Marechal Juin,

14050 Caen Cedex, France

ABSTRACT

Crystalline powders of the super α_2 -Ti3Al alloy were ball milled in a vibrating frame ball milling apparatus in air. Microscopic and X-ray analyses of the as-received powder particles showed the existence of two main phases in the alloy, the α_2 -Ti3Al phase and the B2-Ti₂AlNb phase. Initially, ball milling induces an order-disorder transformation of the α_2 -Ti3Al phase and a severe reduction of the grain sizes. Later the crystalline state of the disordered α -Ti₃Al is partially destroyed, while the B2 ordered Ti₂AlNb phase retains its nanocrystalline structure. As the process advances, a partial recrystallisation of the amorphised phase occurs, starting with the formation of nanocrystals and later single crystal particles. The new structure belongs to the rhombohedral crystal system with lattice parameters that are close to those of α -alumina. This structural transformation is attributed to a ball milling driven oxidation mechanism, where the oxygen of the native oxide of the powder surface is progressively incorporated in the alloy matrix forming metastable Ti rich Al₂O₃ oxides.

INTRODUCTION

Titanium aluminides and their alloys are materials that have drawn much attention in recent years, due to the excellent mechanical properties that they present in high temperature aerospace applications /1-4/. The increasing demand for potential high performance materials at elevated temperatures resulted in the development of new manufacturing processes for high temperature alloys. Conventional metallurgical methods could not always achieve a satisfactory and homogeneous dispersion of the elements of a composite material. Ball milling is a dry, high energy process that produces, in a relatively simple way, complex metal alloy powders with controlled and refined microstructures. Furthermore, by controlling the parameters of this repeated fracturing process nanostructured or even

amorphous materials could be fabricated. The final products made of this method, however, are not completely free of structural inhomogeneities /5-11/.

Experiments conducted in planetary ball mills, in inert gas atmospheres, on a mixture of elemental Ti, Al and Nb powders or on prealloyed Ti-Al-Nb powders showed the formation of new phases (B2/bcc phase, O/orthorhombic phase) that are shown to improve the ductility and the fracture toughness of this type of alloys /12,13/. A crystalline fcc TiN phase is also reported /12/ to appear after the amorphisation of both binary Ti-Al and ternary Ti-Al-Nb alloys. The formation of new phases and the microstructural evolution of prealloyed powders of these systems are not yet clarified, since they seem to be strongly dependent on the ball milling and environmental conditions. In our study, a structural characterisation of the multiphase super $\alpha_2 Ti_3 Al$ alloy is presented after ball milling in a vibratory frame ball mill and the results are compared to those of the planetary one. A 100:1 ball to powder ratio is used in order to induce heavy deformation and accelerate the emerging structural changes. Furthermore, we have used native atmosphere investigating the effects of oxidation on the ball milled microstructures and compared them to the oxidation behaviour of the arc-melted $Ti_3 Al$ alloy /14,15/. For our analysis we have used Scanning Electron Microscopy (SEM), Transmission Electron Microscopy (TEM), High Resolution Electron Microscopy (HREM), and X-Ray Diffraction (XRD) analysis.

EXPERIMENTAL DETAILS

The as-received super α₂-Ti₃Al alloy is manufactured by the Interdisciplinary Research Centre (IRC) for Materials in Birmingham (UK) with a nominal composition of 63 Ti, 21 Al, 12 Nb, 3 v and 1 Mo (at %). The manufacturing process involves rotating disk atomisation, where molten metal impinges onto the surface of a rapidly spinning disk. The liquid metal is mechanically atomised and thrown off the edges of the spinning disk. Solidification of the emerging particles occurs in flight and can be enhanced by a stream of helium. Since this process produces an inhomogeneous multiphase alloy, ball milling is expected to improve the dispersion of the microstructural elements. The as-received powders were ball milled in a vibratory ball mill, "Pulverisette O" Fritsch, for continuous time periods lasting from 2 hours to 108 hours, keeping the vibration amplitude constant. A WC ball of 1 kg (ball to powder ratio 100:1) was used for the ball milling. In order to have TEM specimens, the ball milled powders were mixed with epoxy resin and then were mechanically polished and finally ion-etched. SEM observations were performed in a Jeol JEM 840 electron microscope. Microscopic and atomic scale observations were carried out in a Jeol JEM 120CX TEM microscope operating at 120 kV and a Topcon 002B HREM microscope operating at 200 kV, respectively. X-ray diffraction spectra were obtained by a Siemens D500 diffractometer, using Cu- K_{α} radiation, over the angular range 2θ = 10°-80° in steps of 0.02° (2θ) and counting time 10 s/step.

RESULTS

The powder particles of the as-received material possess a spherical morphology with particle sizes between 90 μm and 120 μm , each one containing several grains with average grain size of 10 μm to 20 μm . X-ray analysis shows that the particles consist of two main phases, namely: the ordered α_2 phase of Ti₃Al and a B2 (ordered β) phase having the composition Ti₂AlNb /16-18/, as depicted in Figure 1 – curve a. There are also a few weak peaks that appear to correspond to the orthorhombic O-phase /18/. SEM observations show that, after the first few hours of ball milling, the powder particles lose their original spherical morphology. Cold welding of broken particle pieces and flakes with larger particles occurs simultaneously. After 24 hours of ball milling most of the as-received powder particles are broken in small pieces with average sizes that do not exceed 15 μ m. As the process of ball milling continues, the particle sizes diminish until an equilibrium between fracturing, welding and refracturing of the powder particles is reached. After approximately 84 h of ball milling the average particle size stabilises to 1 μ m and this does not change until the end of the procedure at 108 h. Small particles ball milled for over 100 h regain the spherical morphology, due to the prolonged mechanical attrition.

The electron diffraction analysis reveals some interesting phenomena that are not detected explicitly

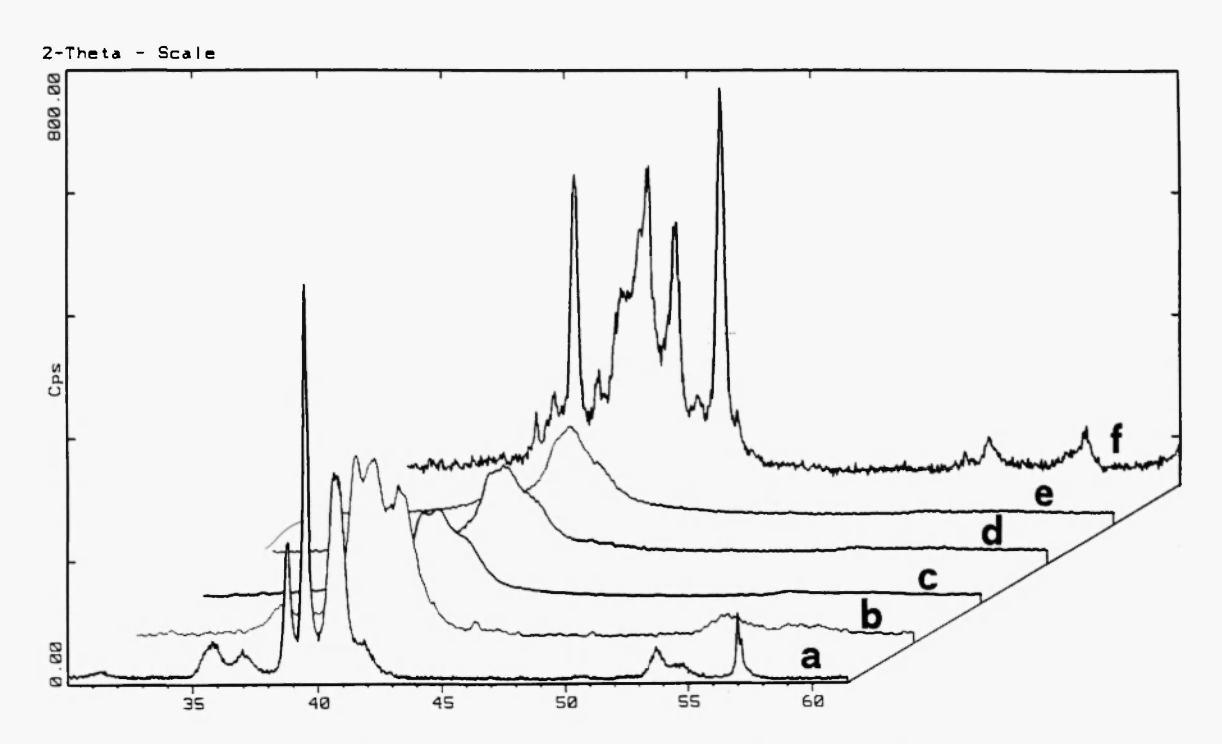


Fig. 1: Multiple X-ray diffraction pattern showing the evolution of the crystal structure of the alloy. The curves correspond to: (a) as-received material, (b) 12 h ball milled material, (c) 48 h ball milled material, (d) 60 h ball milled material, (e) 72 h ball milled material and (f) 108 h ball milled material, respectively.

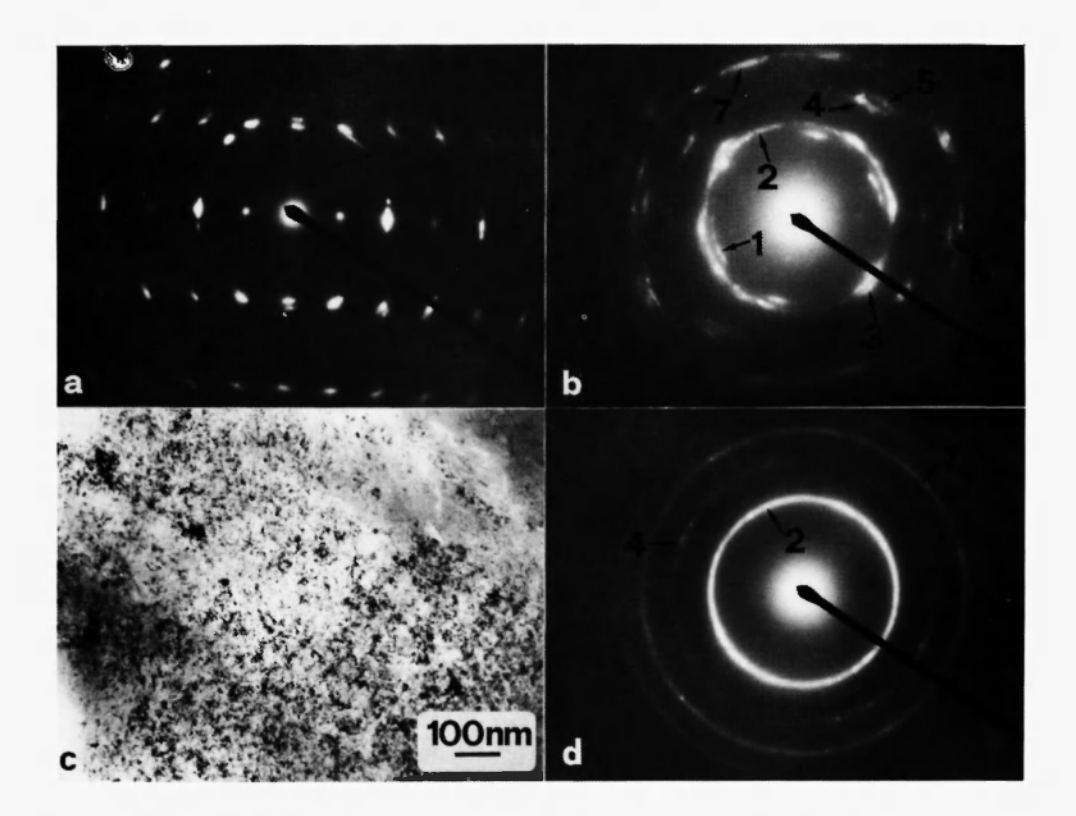


Fig. 2: a) Electron diffraction pattern showing the existence of the DO₁₉ superlattice structure of the α₂-Ti₃Al phase after 32 h of ball milling. b) Diffraction pattern from another area of the 32 h specimen depicting the polycrystalline nature of the alloy. Rings 1, 2, 3, 4, 5, 6, 7 correspond to the disordered α-Ti₃Al, whereas rings 2, 4, 7 also correspond to the ordered Ti₂AlNb phase.
c) TEM micrograph of the 60 h ball milled specimen. A microcrystalline morphology is depicted. d) Corresponding diffraction pattern of Fig. 2c, where rings 1, 3, 5, 6 are absent indicating an amorphisation of the α-Ti₃Al phase.

by SEM and XRD analysis. Electron diffraction patterns taken at 36 h of ball milling show that some of the grains retain the original DO₁₉ superlattice structure (Fig. 2a), whereas the rest of the grains begin to present a polycrystalline structure, as was expected from the fracturing process (Fig. 2b). The complex diffraction pattern of Figure 2b appears to be a superposition of the disordered α phase of Ti₃Al (rings 1, 2, 3, 4, 5, 6, 7) and the ordered B2 phase of Ti₂AlNb (rings 2, 4, 7) ring patterns. Thus, we observe an order-disorder phase transformation, induced by ball milling, during the deformation and fracturing of the grains. This transformation occurs only to one of the two main phases of the original alloy, whereas the B2 phase remains ordered. At 60 h of ball milling the alloy has been completely transformed into homogeneous nanocrystalline materials, depicted in Figure 2c, with grain sizes of the order of 20 nm. Ring (1) of the previous case, corresponding to the $10\overline{10}$ of α -Ti₃Al, is absent in the 60 h specimen (Fig. 2d), whereas the strongest ring of the present diffraction pattern

corresponds to the 110 of the B2 phase. The X-ray analysis of a specimen ball milled for 60 h (Fig. 1 – curve d) shows the main peaks of the α phase of Ti₃Al and of the B2 phase lowered in intensity and significantly broadened in respect to those in the XRD pattern of the as-received material. Combining this result with the electron diffraction observations, it is deduced that the α -Ti₃Al phase of the alloy has suffered a partial amorphisation, whereas the B2 phase still remains nanocrystalline. After 84 h of ball milling, specimens observed in conventional TEM do not show any apparent structural difference from the 60 h specimen, except for the fact that the grain sizes of the B2 phase are reduced to an average diameter of 10 nm. However, employing high resolution electron microscopy in the 84 h specimen, we have observed nuclei of a new crystalline phase in the alloy matrix different from the phases of the original material (Fig. 3a). Fast Fourier transform (FFT) showed that, at first approximation, the new phase possesses a distorted fcc lattice; this was later confirmed by electron diffraction. At 96 h of ball milling the amorphisation of the α phase has advanced and amorphous grains are observed

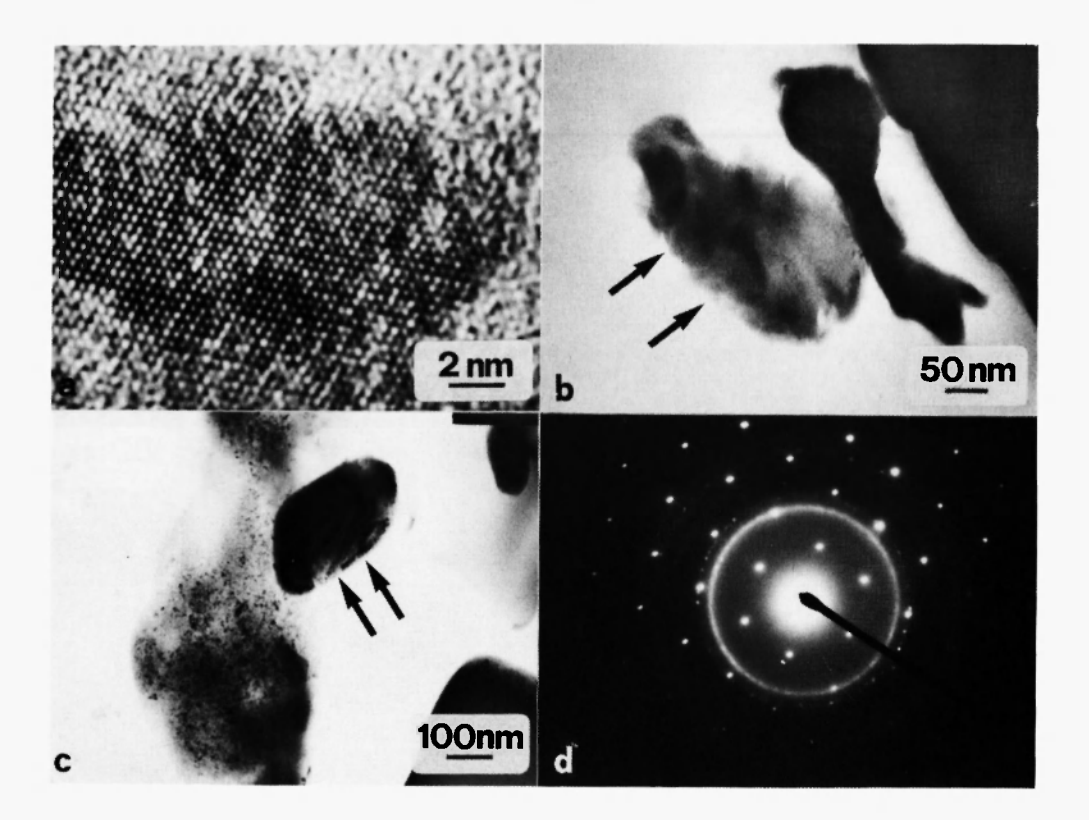


Fig. 3: a) HREM micrograph revealing the growth of a nucleus of new material at the 84 h ball milled specimen. b) An amorphous α-Ti₃Al grain (indicated by arrows) is observed together with a nanocrystalline Ti₂AlNb grain, at 96 h of ball milling. c) The nuclei of Fig. 3a have grown into microparticles (indicated by arrows) after 102 h of ball milling. d) Corresponding diffraction pattern of Fig. 3c showing the coexistence of the nanocrystalline Ti₂AlNb phase with the single crystalline form of the new phase.

together with grains of the B2 phase of Ti_2AlNb (Fig. 3b). At 102 h the nuclei of the new phase have grown into microparticles, of the order of 0.3 μm , coexisting with the nanocrystalline B2 phase of Ti_2AlNb and the nearly amorphous α - Ti_3Al phase (Fig. 3c). The single crystalline part of the corresponding diffraction pattern of Figure 3c (Fig. 3d) matches perfectly with the FFT of Figure 3a, confirming that nuclei and microparticles are of the same phase. TEM micrographs and the XRD pattern received after 108 h of ball milling (Fig. 1 – curve f) showed that the microparticles of the new phase, with grain sizes between 0.1 μm and 0.8 μm , become one of the main phases in the alloy together with the α phase of Ti_3Al and the B2 phase of Ti_2AlNb , while the originally observed orthorhombic phase is still present. In Figure 4a and 4b a particle of the new phase consisting of two grains is depicted, showing the existence of a twin interface inside the particle that is grown by mechanical deformation of the particle due to ball milling.

The crystallographic analysis of the electron diffraction patterns, shown in Figures 4c and 4d, and the X-ray diffraction patterns of the new phase resulted in the following: the new phase crystallises in the rhombohedral crystal system, with space group R3 or R3, and possesses a primitive unit cell with

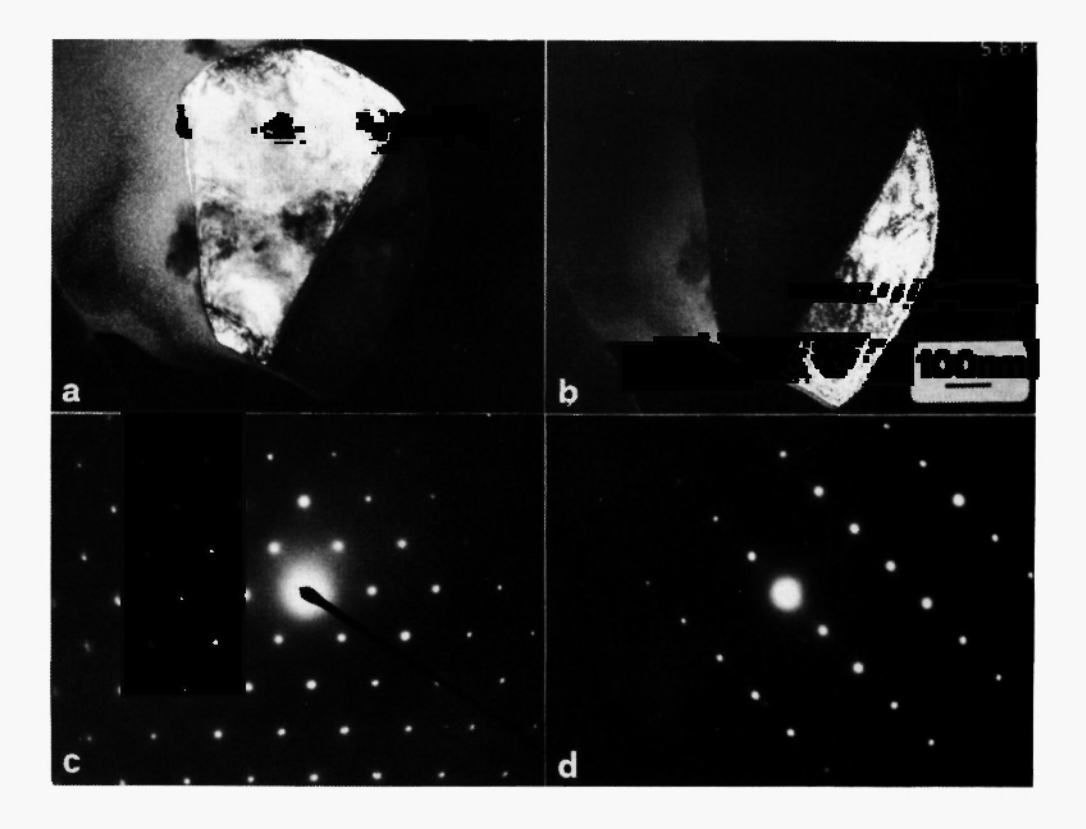


Fig. 4: a) Dark field (DF) image of a particle of the new phase that contains an interface, after 108 h of ball milling. b) DF image of the other grain of the bicrystal. c) Diffraction pattern of the new phase with the [0111] zone axis oriented parallel to the electron beam. d) Diffraction pattern of the new phase with the [3300] zone axis oriented parallel to the electron beam.

a = 0.504 nm and α = 56.4°. This structure can also be described either by a hexagonal unit cell with a = 0.476 nm and c = 1.267 nm, or a distorted fcc unit cell with a = 0.693 nm and α = β = γ = 86.8°. The X-ray results of the crystallographic indexing of the new phase reflections observed in Figure 1 – curve f, along with the experimental (d exp-XRD) and calculated (d calc-XRD) interplanar spacings and the relative intensity I/I_o values are summarised in Table 1. The experimental interplanar spacings (d exp-TEM) derived from the electron diffractions are also depicted in Table 1.

The calculated and c lattice constants and the crystal system indicate that the new phase has parameters that are close to those of crystalline α -Al₂O₃. The XRD intensities, however, are different from those of α -alumina implying that in the produced new phase there is a mixture of Al and Ti in the cationic sites of the lattice and the new phase could be more correctly described as Ti rich α -alumina. The structural evolution of the main phases of the alloy as a function of milling time is schematically depicted in Table 2.

Table 1

	hkl	hkil	d exp-TEM	d exp-XRD	d cale-XRD	LI_{o}
	(rhomb.)	(hexag.)	(nm)	(nm)	(nm)	
1	110	0112	0.346	0.34700	0.34547	9
2	211	1014	0.252	0.25120	0.25116	16
3	101	1120	0.237	0.23815	0.23794	29
4	222	0006	0.213	0.21153	0.21120	100
5	210	1123	0.208	0.20829	0.20731	18
6	311	2025	0.161	0.16008	0.15988	15
7	211	1232	0.152	0.15081	0.15126	11
8	333	0009	0.140	0.14059	0.14080	8
9	211	3030	0.137	0.13723	0.13737	9
10	300	3033	0.131	0.13075	0.13064	15

Table 2

Milling time (h)	0	36	60	84 → 108
Main phases of	α ₂ -Ti ₃ Al +	α-Ti ₃ Al +	amorphous +	amorphous +
the alloy	B2/bcc	B2/bcc	B2/bcc	B2/bcc +
				rhombohedral

DISCUSSION

The deformation mechanism that is induced by the ball milling combined with the presence of atmospheric oxygen leads to a series of structural transformations of the alloy phases.

A. The α_2 -Ti₃AI phase

The hcp α_2 phase of Ti₃Al is present in the as-received material exhibiting an ordered DO₁₉ superlattice structure. During the ball milling process, due to the repeated fracturing and deformation of the powder particles, the ordering of this phase is gradually destroyed and finally transforms into disordered polycrystalline α -Ti₃Al. Although the mechanical impact gives rise to higher temperatures at a local level the α_2 -to-O (orthorhombic) phase transformation /14/ was not observed. The polycrystalline α -Ti₃Al is progressively transformed into amorphous material coexisting with the crystalline B2-Ti₂AlNb phase. The ball milling driven incorporation of oxygen, that is present in the native oxide, results in a recrystallisation of the amorphous phase and growth of nuclei of rhombohedral single crystalline oxides, a phenomenon that is compatible with high temperature oxidation of ternary Ti-Al-Nb alloys /15/. Nuclei of the new phase grow into microparticles that become one of the main phases of the ball milled product.

B. The B2-Ti₂AlNb phase

The ordered B2-Ti₂AlNb phase is also present in the as-received material and possesses a bcc structure. Unlike the α_2 phase of Ti₃Al, the B2 phase remains stable during the ball milling, retaining its ordered crystalline structure. It has been shown that the B2 phase becomes amorphous after ball milling in planetary ball milling systems and then recrystallises into an fcc phase /12,13/. None of these transformations was observed in our case, where the B2 phase suffered only a reduction of grain sizes and was still nanocrystalline at the end of the process. This could be attributed to the higher ductility that the B2 phase presents in comparison to that of the α_2 phase. Additionally, the quantity of the O phase, that originates from transformation of the B2 phase /12/, remained constant throughout the process. This indicates that during our process no phase transformation occurred in the B2-Ti₂AlNb phase.

C. The rhombohedral phase

The formation of this phase, resulting from the recrystallisation of the amorphous α -Ti₃Al could be explained by the following mechanism: The oxygen of the atmosphere creates a native oxide around the powder particles, which is progressively incorporated into the material through the continuous welding that ball milling induces. Due to the local rise of temperature, the embedded oxygen reacts with the Ti and Al atoms, forming nuclei of stable crystalline oxides. Some of the Al atoms of the

oxides could be substituted by Ti or vice versa, resulting in minor changes of lattice constants. Later in the process, the nuclei grow into larger particles that do not seem to be affected by further incorporation or absorption of oxygen. This is supported by the fact that electron diffraction analysis shows identical patterns from the formation of the nuclei of the new phase until the end of the process. The Ti-rich α -alumina product of this ball milling driven oxidation mechanism is also formed during high temperature oxidation of Ti₃Al aluminides, where the Nb content promotes its formation /15/. No other crystalline oxide was detected in this study.

CONCLUSION

Powders of the multiphase super α_2 -Ti₃Al alloy were processed in a vibrating frame ball milling apparatus, in native atmosphere. The powder particles were morphologically and analytically investigated by SEM and structurally by XRD and TEM. The following important stages were observed progressively during the ball milling: Primarily, the α_2 -Ti₃Al phase suffers a disruption of ordering, while the grain sizes diminish. At the second stage, the crystalline state of the disordered α -Ti₃Al is destroyed and becomes partially amorphous, whereas the B2 ordered Ti₂AlNb phase retains its crystalline structure. At the third stage, a recrystallisation of the amorphous phase occurs, beginning with the formation of nanocrystals and later single crystal particles. The new structure is rhombohedral with lattice parameters that are near to those of α -alumina. This phenomenon is explained by a mechanism of incorporation of oxygen from the native oxide and its reaction due to elevated local temperature with Ti and Al atoms, driven by the continuous deformation and welding of powder particles during the ball milling process.

ACKNOWLEDGEMENTS

This work is supported by the program PENED 95-1504 of the Greek Secretariat of Research and Technology. The authors wish to thank the IRC Deputy Director Dr. M.H. Jacobs for providing the original material and Dr. V. Pontikis for valuable discussions and comments.

REFERENCES

- 1. F.H. Froes, C. Suryanarayana and D. Eliezer, J. Mater. Sci., 27, 5113 (1992).
- 2. C. Suryanarayana and F.H. Froes, Nanstruct. Mater., 1, 191 (1992).
- 3. M. Oehring, T. Klassen and R. Bormann, J. Mater. Res., 8, 2819 (1993).
- 4. H. Chang, H.J. Hofler, C.J. Altstetter and R.S. Averback, *Scripta Metall. et Mater.*, 25, 1161 (1991).

- 5. A.W. Weeber, A.J.H. Wester, W.J. Haag and H. Bakker, *Physica*, 145B, 349 (1987).
- 6. J. Eckert, L. Schultz and K. Urban, J. Mater. Sci., 26, 441 (1991).
- 7. M. Oehring and R. Bormann, *Mater. Sci. Eng. A*, 134, 1330 (1991).
- 8. G.B. Schaffer, Scripta Metall. et Mater., 27, 1 (1992).
- 9. C.C. Koch, Nanostruct. Mater., 2, 109 (1993).
- 10. Th. Kehagias, L. Coheur and P. Delavignette, Mater. Sci. Eng. A, 131, 1 (1991).
- 11. Th. Kehagias, L. Coheur and P. Delavignette, J. Mater. Sci. Lett., 12, 1059 (1993).
- 12. Guo-Hao Chen, C. Suryanarayana and F.H. Froes, Metall. Mater. Trans. A, 26A, 1279 (1995).
- 13. C. Suryanarayana, G.E. Korth and F.H. Froes, Metall. Mater. Trans. A, 28A, 293 (1997).
- 14. K. Muraleedharan, D. Banerjee, S. Banerjee and S. Lele, Phil. Mag. A, 71, 1011 (1995).
- 15. T.K. Roy, R. Balasubramaniam and A. Ghosh, Metall. Mater. Trans. A, 27A, 3993 (1996).
- 16. D.G. Konitzer, I.P. Jones and H.L. Fraser, Scripta Metall., 20, 265 (1986).
- 17. D. Banerjee, T.K. Nandy and A.K. Gogia, Scripta Metall., 21, 597 (1987).
- 18. G. Itoh, T.T. Cheng and M.H. Loretto, Mater. Trans. JIM, 35, 501 (1994).